Research Article

Mussel inspired durable pH-responsive mesh for high-efficient oil/water separation

Yijing Wang[1] · Ling Jin[1] · Tao Xue[1] · Feifei Shao[1] · Yuan Yao[1] · Xinxin Li[1]

Abstract

The application of pH-responsive superwetting materials receives increasing attention in oil/water separation. In this work, a mussel inspired robust surface coating fabricated with dopamine, copolymer PDMAEMA-*co*-PHEMA-*co*-PHFBMA (PDHH) and SiO_2 nanoparticles (DPS) was formed on stainless steel mesh to perform multiple repeatable oil/water separation. Herein, dopamine was chosen to provide strong adhesion strength and durability, endowing the mesh excellent stability in harsh environments, such as mechanical abrasion, acid/alkali immersion and UV irradiation. In virtue of pH stimulation, the as-prepared mesh can be reversibly switched between superhydrophobicity and superhydrophilicity. Moreover, the mesh possesses remarkable oil/water separation efficiency (SE) (≥98%) and desirable recyclability. An oil collector prepared by the mesh and kapok fiber showed good oil absorption capability in the range of 39.67–79.56 g/g. The facile and inexpensive preparation of the durable separation device enables it promising in actual oil/water separation.
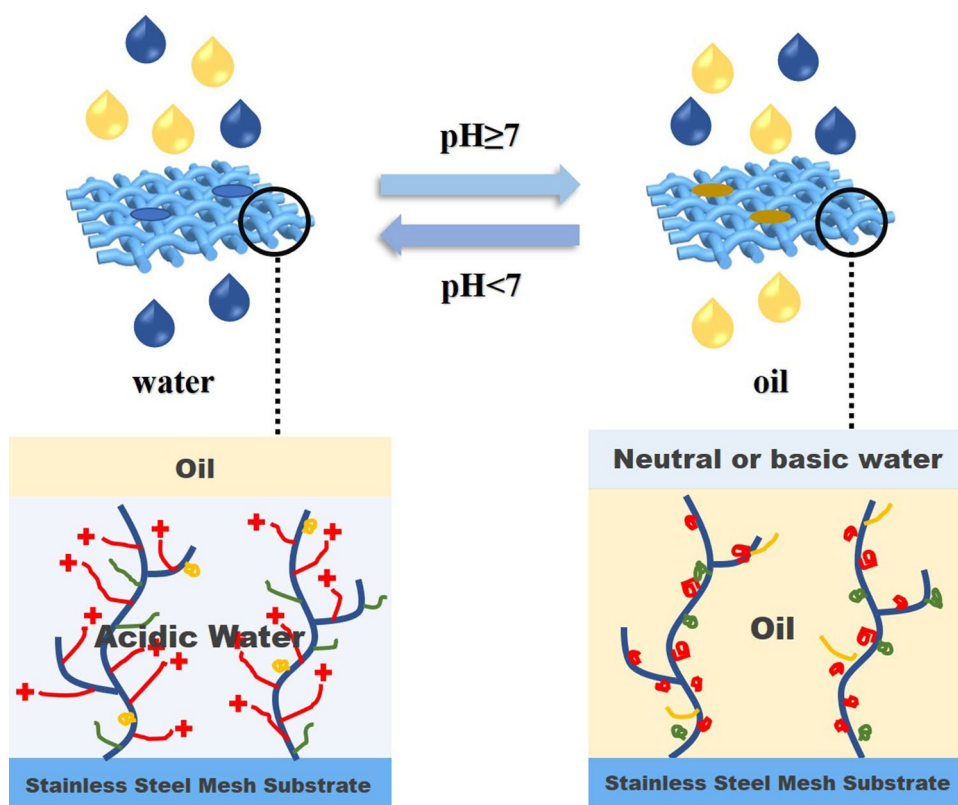

✉ Xinxin Li, xinxinli@ecust.edu.cn | [1]Key Laboratory of Specially Functional Polymeric Materials and Related Technology, Ministry of Education, School of Materials Science and Engineering, East China University of Science and Technology, Shanghai 200237, China.

Graphic abstract

1 Introduction

With the rapid development of industrialization, worldwide oil spill and industrial oily wastewater have discharged various toxic compounds to the water systems and thus threaten the global ecosystem [1, 2]. Superwetting materials, showing different interfacial effects on oil and water, are effective means for oil/water separation [3–10]. For the purpose of separating the contaminants and pure water with higher flexibility, smart response of superwetting materials become the most promising matter since their surface structure could alternate under external stimuli such as pH [11–15], light [16–18], temperature [19, 20], electric field [21, 22], gas [23] and pressure [24]. Their stimuli-responsive behavior can result in switchable wettability between superhydrophobicity and superhydrophilicity, offering different affinity to water and oily matters during the separation.

Among these smart switchable materials, pH-responsive superwetting materials with porous structures have great advantages on convenient operation, rapid response and uncomplicated equipment [25–28]. Generally, the pH-responsibility comes from polymeric coatings that can reversibly switch their chemical conformation or polarity to change the surface energy and surface wettability [29–31]. Zhang et al. [30] grafted pH-sensitive poly(2-vinylpyridine)-based block copolymer on non-woven textiles and polyurethane sponges. The resulted material realized switchable superoleophilicity and superoleophobicity and exhibited excellent oil/water separation performance. Dai [32] fabricated a three-dimensional structural collagen fiber matrix modified by poly(methacrylic acid-*co*-glycidyl methacrylate) copolymer. The functional material can be tuned to absorb or release oil with pH variation, which is beneficial for recycling the absorbed oil. Yi [33] developed a novel membrane based on reduced graphene oxide and polyacrylic acid (PAA) grafted carbon nanotube. Benefited from the pH-responsive property of PAA, the pore size of the membrane can be narrowed in acid solution and enlarged in basic solution, providing controllable separation efficiency (SE) over a wide pH range. However, the layer of functional polymer is intolerant toward acids, bases and organic solvents, and microscale/nanoscale rough structures on surface are inevitably weak towards

Scheme 1 Schematic illustration of the preparation of DPS stainless steel mesh
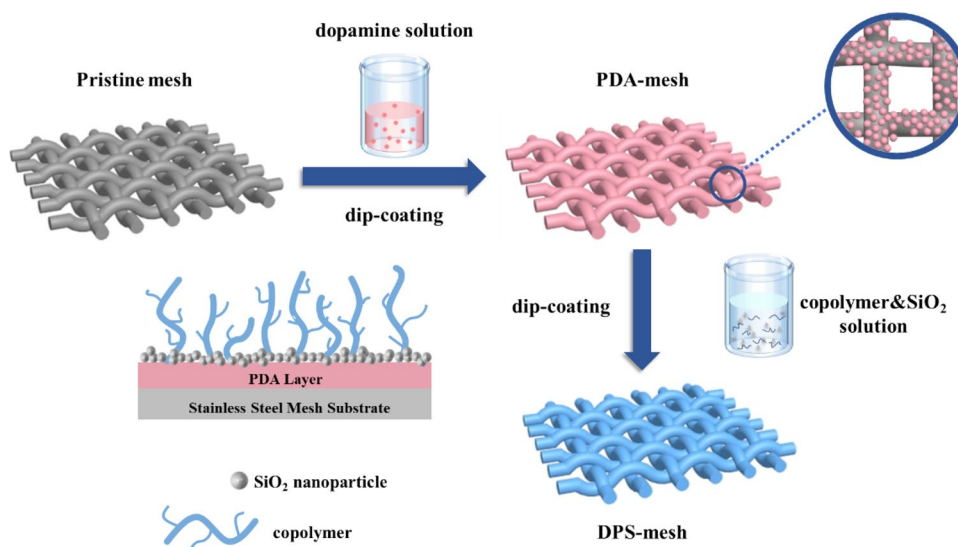
mechanical abrasion [34]. The low stability of pH-responsive materials limits their application in practical oil/water separation and can be further optimized.

Mussel-inspired chemistry provides a facile and promising surface-modification approach to introduce special wettability behavior and hierarchical structures onto surfaces [35–39]. Polydopamine (PDA) is quite similar in molecular structure to the dihydroxyphenylalanine in mussel foot proteins. It has been proved to show strong adhesive ability on nearly all kinds of substrates, offering new opportunities in oil/water separation [40–44]. Huang [45] used PDA as a small molecular bioadhesive to prepared the superhydrophobic polyurethane sponge with hierarchically structured surface. The as-prepared sponge remained excellent absorption capacities towards pump oil and chloroform after five absorption cycles. Kang [46] presented a durable superhydrophobic glass wool (GW) fabricated by the combination of PDA chemistry and chemical vapor deposition of polydimethylsiloxane. The water contact angle (WCA) of the superhydrophobic GW remained above 150° after being kept in diesel and petrol for even 30 days. This was attributed to the inherent stability of the PDA nanoparticles towards oil.

Herein, we described a facile method to fabricate a random copolymer-coated stainless steel mesh with pH-switchable wettability to efficiently separate oil/water mixture, as illustrated in Scheme 1. The dopamine@polymer@SiO$_2$ nanoparticles (DPS) stainless steel mesh was fabricated by dipping meshes into dopamine solution and then treated with the mixture solution of poly(2-(dimethylamino) ethyl methacrylate)-*co*-poly(2-hydroxyethyl methacrylate)-*co*-poly(2,2,3,4,4,4-hexafluorobutyl methacrylate) (PDMAEMA-*co*-PHEMA-*co*-PHFBMA) and SiO$_2$ nanoparticles. Stainless steel mesh was chosen for its high compressive strength, corrosion resistance and

firmness to provide efficient and durable foundation for oil/water separation. In our previous work, the functional copolymer was synthesized by simple free radical polymerization [47, 48]. PDMAEMA segments gave the pH responsiveness, HEMA segments rose the hydrophilicity and the HFBMA segments reduced surface energy. PDA enhanced the adhesion between the components and SiO$_2$ nanoparticle provided the required surface roughness. The as-prepared meshes exhibited intelligent pH-switchable wettability, excellent mechanical and chemical stability. The microstructure and surface properties of the DPS stainless steel meshes were investigated and the oil–water SE and recyclability of the mesh were evaluated. The mussel inspired durable pH-responsive mesh is promising in high-efficient oil/water separation.

2 Experimental

2.1 Materials

2-(Dimethylamino) ethyl methacrylate (DMAEMA), 2-hydroxyethyl methacrylate (HEMA), and 2,2,3,4,4,4-hexafluorobutyl methacrylate (HFBMA) were purchased from Aladdin Biochemistry Co. Ltd. and were filtered to remove the inhibitor through alkaline alumina column for further use. Dopamine hydrochloride (98.0%) was purchased from Aldrich Chemical Company. Silica nanoparticles (7–40 nm) and 2,2'-azobis-(isobutyronitrile) (AIBN) were purchased from Macklin Biochemistry Co. Ltd. The stainless steel meshes (500 mesh size) were obtained from Shanghai Jiya Industrial Wire Mesh Products Co., Ltd. Meshes were washed with acetone, ethanol, and deionized water in sequence under ultrasonication to remove impurities and dried at 60 °C for 24 h. Kapok fiber was purchased from

Nanning Weiyu Home Textile Co., Ltd. It was immersed into ethanol under ultrasonication and dried up for later use. Other reagents were used without further purification.

2.2 Synthesis of PDMAEMA-*co*-PHEMA-*co*-PHFBMA

Copolymer PDMAEMA-*co*-PHEMA-*co*-PHFBMA (PDHH) was synthesized through free radical polymerization with following details. A mixture of DMAEMA (12.59 g), HEMA (2.60 g), HFBMA (5.00 g), and AIBN (0.16 g) were dissolved in purified toluene (100 mL) under ultrasonication and then poured into a dry eggplant-type flask with a magnetic stirrer. The system was removed oxygen by nitrogen gas for 0.5 h and stirred for another 4 h with a thermostat at 65 ℃ under nitrogen protection. The obtained copolymer was precipitated into excessive *n*-hexane for three times and then dried under vacuum oven at 65 ℃.

2.3 Preparation of PDA modified stainless steel mesh

Dopamine hydrochloride was dissolved in deionized water to prepare a solution with a mass concentration of 2 g/L and Tris buffer was used to adjust solution pH to 8.5. The stainless steel mesh was immersed in the solution for 0.5 h under ultrasonication and then stirred for 24 h. After reaction, the PDA mesh was washed by ethanol and water for several times and was dried in oven at 60 ℃.

2.4 Fabrication of the dopamine@polymer@ SiO$_2$-coated (DPS) stainless steel mesh

Silica nanoparticles (THF, 1 wt%) and copolymer PDHH were dispersed into tetrahydrofuran to form a coating solution. The DPS mesh was prepared by immersing the PDA mesh into the solution for 0.5 h. The DPS mesh was dried in a vacuum oven at 120 ℃ for 3 h. Finally, after washing in ethanol to remove residuals, the mesh was dried at 60 ℃. In addition, a coated mesh without being modified with dopamine was prepared as polymer@SiO$_2$-coated (PS) stainless steel mesh for comparison.

2.5 Fabrication of oil collector

1.0 g NaClO$_2$ was ultrasonically dissolved in 100 mL deionized water, and acetic acid was added dropwise with a syringe until the solution pH was adjusted to 4.5. Then, 1.0 g kapok fiber was added and was poured into a single-neck flask equipped with a mechanical stirrer. The reaction was stirred at 650 rpm and 80 ℃ for 2 h. After the reaction, the fibers were washed with deionized water until the pH value of the filtrate reached 7. The DPS stainless steel meshes were cut into small rectangle blocks (2×4 cm) and folded into squares (2×2 cm). Pretreated kapok fiber was filled into the stainless steel mesh bag and the oil collector was prepared after the edges were sewed on with fishline.

2.6 Characterization

The morphologies of the as-prepared meshes were observed by scanning electron microscopy (SEM, Hitachi S-3400N). The WCA of as-prepared material surfaces was measured three times by a contact angle measuring instrument (JC2000D2) with 2 μL of liquid at ambient temperature.

2.7 Oil/water separation experiments

The separation capability of the DPS stainless steel mesh was gauged through a simple filtering device. Six different kinds of oil–water mixtures (*n*-hexane, cyclohexane, kerosene, dichloromethane, chloroform and carbon tetrachloride) were prepared by taking same volume of oil and water, using Oil Red O to dye the oil, and mixing the oil and water. The SE and flux of the meshes were calculated according to following equations:

$$SE = \frac{m_1}{m_0} \times 100\%$$

$$Flux = \frac{V}{S \times t}$$

where m$_0$ and m$_1$ are the weight of water or the solvent before and after separation, respectively, V is the volume of the filtrate, S is the effective filtration area, and t is the filtration time.

## 2.8 Oil/solvent absorption capacity

The oil collector was dipped into various solvents or oils until reaching the absorption equilibrium, after that the excess liquid was removed for mass measurement. The measurement process needs to be fast to avoid solvent evaporation. The absorption capacity Q of the oil collector was calculated according to the following equation:

$$Q = \frac{m_1 - m_0}{m_0}$$

2.9 Durability tests

To evaluate the mechanical stability of DPS mesh, a mesh loaded with 100 g weight was put on the abrasive paper with selected roughness (500CW, 1000CW, 1500CW). For each cycle, the mesh was pulled along the ruler for 10 cm.

Fig. 1 Photographs of the acidic water (pH = 1) and alkaline water (pH = 13) on the (**a**) DPS mesh and (**b**) pristine mesh. WCA of the DPS mesh with (**c**) acidic (pH = 1), (**d**) alkaline (pH = 13) water droplets. (**e**) FESEM image of the DPS mesh: magnified 500 times
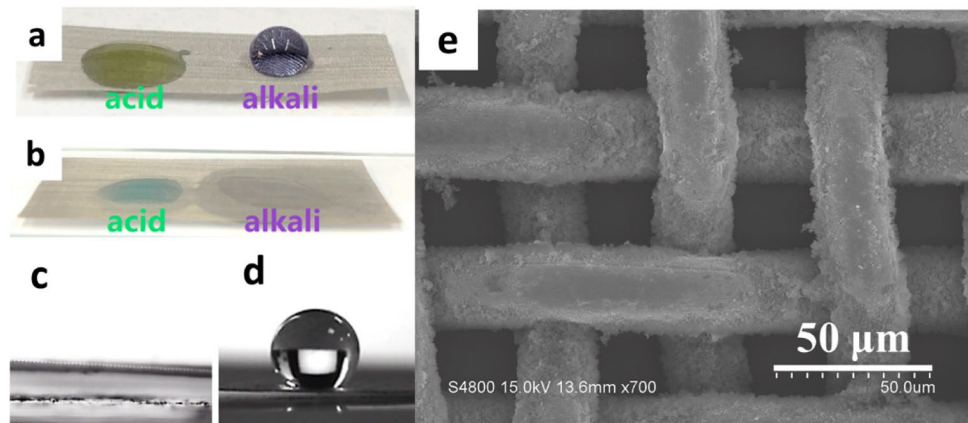
The surface morphology was observed and WCA was recorded after each 5 cycles.

For the acid/alkali resistance test, DPS meshes were immersed into 1 M HCl solution, 1 M NaOH solution, 1 M NaCl solution, hot water, and ice water for 1 h, respectively. After dried in oven at 80 °C, the WCAs were measured and dichloromethane/alkaline water separation performance was evaluated.

In the UV-irradiation resistance test, DPS meshes were treated under UV irradiation for a series of time periods at 25 ± 2 °C with a relative humidity of $60 \pm 2\%$. WCAs were measured once UV irradiation finished and then heavy oil/water separation performance was evaluated as above.

3 Results and discussion

The DPS stainless steel mesh was prepared by dip-coating of stainless steel mesh into PDA solution and copolymer PDHH suspension containing SiO_2, shown in Scheme 1. The copolymer PDHH with pH-responsiveness was synthesized via simple radical polymerization (Fig. S1) [47]. The FT-IR and ^1H NMR spectra (Figs. S2 and S3) indicated that the copolymer has been successfully synthesized.

3.1 Surface morphology and pH-switchable wettability of DPS meshes

The surface wettability and morphology of the DPS mesh were measured to confirm the dip-coating process resulted in the pH-sensitive superwetting surface on meshes. Figure 1a revealed that the DPS mesh was hydrophobic under alkali condition, and turned hydrophilic under acid condition. However, the pristine mesh absorbed all droplets quickly (Fig. 1b) and exhibited nonselective wettability. Acidic water (pH = 1) could be fully absorbed within 10 s by DPS mesh (Fig. 1c). In contrast, the DPS mesh at alkaline water (pH = 13) showed
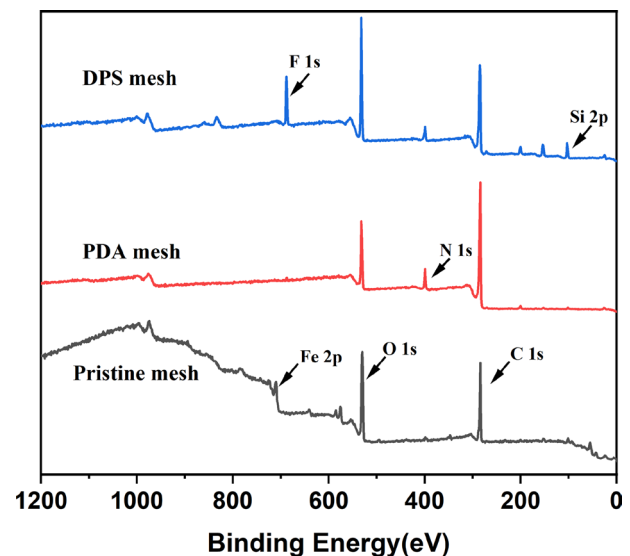

Fig. 2 XPS spectra of three different stainless steel mesh: pristine mesh, PDA mesh and DPS mesh

Table 1 Surface chemical composition of the pristine mesh and PDA mesh from XPS spectra

Sample	C1s/%	O1s/%	N1s/%	N/C	O/C
Pristine mesh	50.3	42.0	3.5	0.069	0.835
PDA (theoretical value)	72.7	18.2	9.1	0.125	0.250
PDA mesh	72.9	18.4	9.0	0.123	0.252

superhydrophobicity with an WCA of 153° (Fig. 1d) due to the pH-responsive surface on the mesh (Fig. 1e). Figure S4 showed the process in which an alkaline water droplet rolled off the DPS mesh with a sliding angle less than 15°.

The surface chemical compositions of three different meshes (pristine mesh, PDA mesh and DPS mesh) were characterized by XPS spectra in Fig. 2. For the pristine mesh, it mainly has the characteristic peaks of C, O and Fe

elements. After modified by PDA, the characteristic peak of the Fe element basically disappeared and was replaced by the appearance of N element at 399 eV from PDA. The N/C and O/C atomic ratios of pristine mesh were 0.069 and 0.835, respectively, whereas the N/C ratio increased to 0.123 and the O/C ratio decreased to 0.252 in PDA mesh (Table 1). The ratios were in good agreement with the theoretical values of PDA which confirms that PDA was uniformly distributed on the mesh.

Moreover, the approximate thickness of dopamine@polymer@SiO$_2$ layer was estimated by Automatic Mercury Porosimeter. The pore diameter before and after the dip coating experiments were 36.12 and 35.48 μm, respectively. The DPS layer was about 0.32 μm.

$$d = \frac{d_1 - d_0}{2}$$

where d_1 is the pore diameter of pristine mesh and d_0 is the pore diameter of the DPS mesh.

To further demonstrate the effect of copolymers on pH-response, PDHH solutions with different concentrations (0.25, 0.5, 1, 2, 3 wt%) were prepared and used to modify the meshes respectively. WCA (Table 2) and surface morphologies (Fig. 3) were characterized for comparison. After modification by PDHH solutions (0.25, 0.5, 1 wt%), a rougher state of surface could be clearly observed due to the uniform distribution of polymer and the surface roughness increased significantly with the rise of concentration. When pH ≥ 7, the WCA increased to 145.6° with the increase of concentration, which was in agreement with the results of FESEM. However, as the concentration of PD$_4$H$_1$H$_1$ solution reached 2 and 3 wt%, solution would flow during the volatilization of THF, eventually formed continuous smooth surface and led to smaller WCA in neutral/alkalic condition. Thus, the concentration of PD$_4$H$_1$H$_1$ was optimized as 1 wt%.

The stability of functional coating surfaces is very important for their practical applications. However, the interaction between the functional coating and substrate is usually not strong enough for general special wetting materials [49]. The PDA layer was introduced to enhance the adhesion strength via the covalent bonds between hydroxyl- and amine-functionalized groups [50–52]. And a coated mesh without dopamine modification was

Table 2 The WCA of stainless steel mesh modified by polymer solution of different concentration

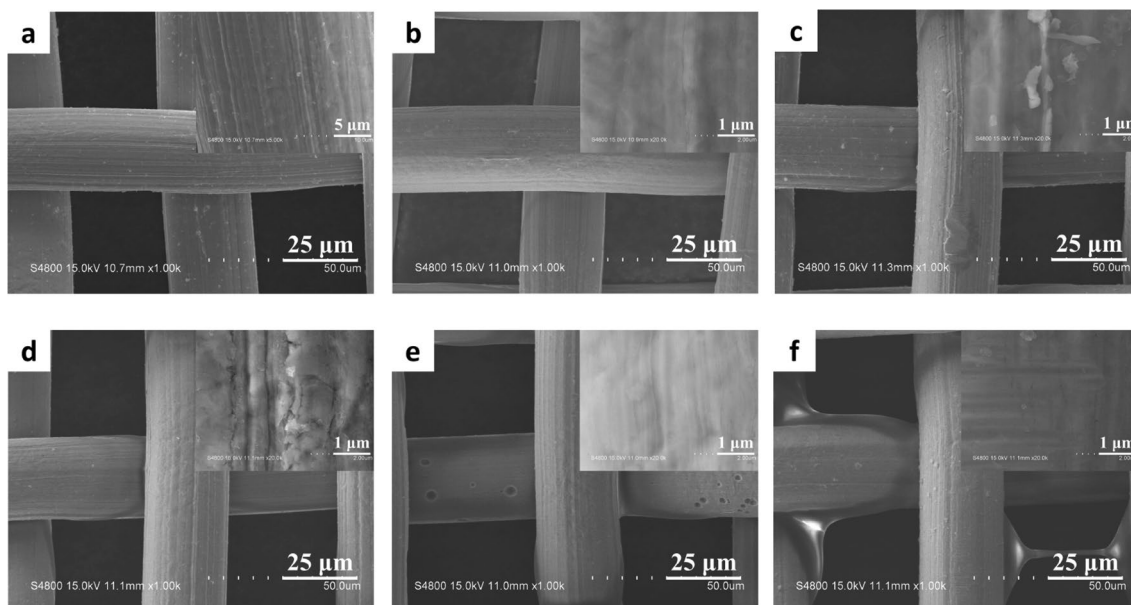| Concentration (wt%)	WCA (°)		
	pH = 1	pH = 7	pH = 13
0	0	0	0
0.25	0	137.8	139.0
0.5	0	141.5	142.0
1	0	146.9	145.6
2	0	116.0	120.5
3	0	121.0	131.5

Fig. 3 FESEM images of the (**a**) non-treated stainless steel mesh and different concentration polymer modified stainless steel mesh, (**b**) 0.25 wt%, (**c**) 0.5 wt%, (**d**) 1 wt%, (**e**) 2 wt%, (**f**) 3 wt%
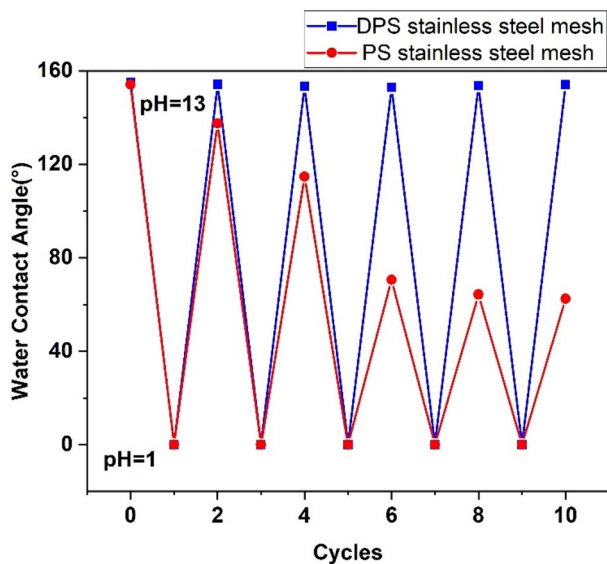
Fig. 4 WCA of DPS mesh and PS mesh for pH conversion cycles between pH = 1 and pH = 13

prepared as PS stainless steel mesh for comparison. As displayed in Fig. S5a, the PDHH copolymer and SiO_2 nanoparticles clumped together and piled up at the intersection of stainless steel wire of PS mesh, nearly blocking the mesh. After preprocessed by PDA, the surface of DPS mesh was covered by uniformly distributed copolymer and SiO_2 nanoparticles (Fig. S5b). Moreover, the DPS mesh showed stable pH responsiveness under reversible cycles between pH = 1 and pH = 13 while the responsive performance of PS mesh decreased after two cycles (Fig. 4).

3.2 Oil/water separation performance of DPS meshes

The separation property of DPS mesh was investigated with sand core filter for different oil/water mixtures, as shown in Fig. 5a, n-hexane/acidic water mixture (1:1, v/v) was slowly poured into the funnel and was driven only by gravity. Acidic water immediately permeated through the DPS mesh and flowed into the flask underneath owing to the superhydrophilicity whereas n-hexane was blocked above the mesh (Video S1). In contrast, when poured the dichloromethane/alkaline water mixture (1:1, v/v) into (Fig. 5b), dichloromethane rapidly passed through the funnel (Video S2). However, the alkaline water was obstructed because the PDMAEMA blocks collapsed in deprotonation process and exhibited high repellency to water in alkali environment. After filtration, oil and water phases were completely separated, and other phases were not presented in the filtrate.

During the separation, the filtering time and liquid weight (before and after separation) were recorded, respectively. Therefore, the SE and flux of the DPS mesh for different organic oil pollutants were calculated. As shown in Fig. 5c, d, the SE of the meshes were all above 98% for various immiscible oil/water mixtures with only slight differences due to the density of oils. After each separation, the meshes were washed with ethanol and then dried for reuse. To evaluate the recyclability of the as-prepared meshes, the separation with the n-hexane/acidic water and carbon tetrachloride/alkaline water mixture were taken for examples (Fig. 5e, f). After ten cycles of separation, the SE of the DPS meshes were above 97% and fluxes were more than 1×10^4 L m^{-2} h^{-1}.

PS mesh was also tested with n-hexane/acidic water mixture for comparison. In the second cycle, the SE decreased from 97% to 92%. The oil phase and the water phase could not be separated completely and the flux increased apparently in the next cycle due to the weak adhesion between the coating and the mesh. As displayed in Fig. 6a, b, the micro-nano rough structures on the surface of the DPS mesh still existed after ten cycles and showed little difference with the original DPS mesh. On the contrary, few SiO_2 nanoparticles remained on the surface of PS mesh after three cycles (see Fig. 6c, d). The layer of copolymer and SiO_2 nanoparticles was obviously peeled off, which reduced the surface roughness and changed pore size, causing the poor SE and increase of flux. These results well proved that the DPS mesh possesses favorable recyclable property.

3.3 Durability of DPS meshes in harsh environments

The durability of oil/water separating meshes in harsh environments, such as mechanical abrasion, acid/alkali immersion and UV irradiation, is required in practical applications. A simple abrasion (Fig. S6) test was performed with abrasive papers (500CW, 1000CW, 1500CW) to evaluate the mechanical stability of DPS mesh. The relationship between pH-switchable behavior and sliding distance was displayed in Fig. 7.

The surface structures on the mesh were destroyed to various degree after repeated abrasion. The three dimensional braided structure of the stainless steel mesh and the PDA layer protected hierarchical structures almost kept inside the DPS mesh (Fig. 8a) whereas the surface of PS mesh underwent a serious damage (Fig. 8b). The WCA under alkaline conditions gradually declined with the increase of the sandpaper roughness and the sliding distance, nevertheless, the DPS mesh was still pH-switchable and superhydrophobic with a WCA of 150 ± 0.5° even after 40 cycles of abrasion test.
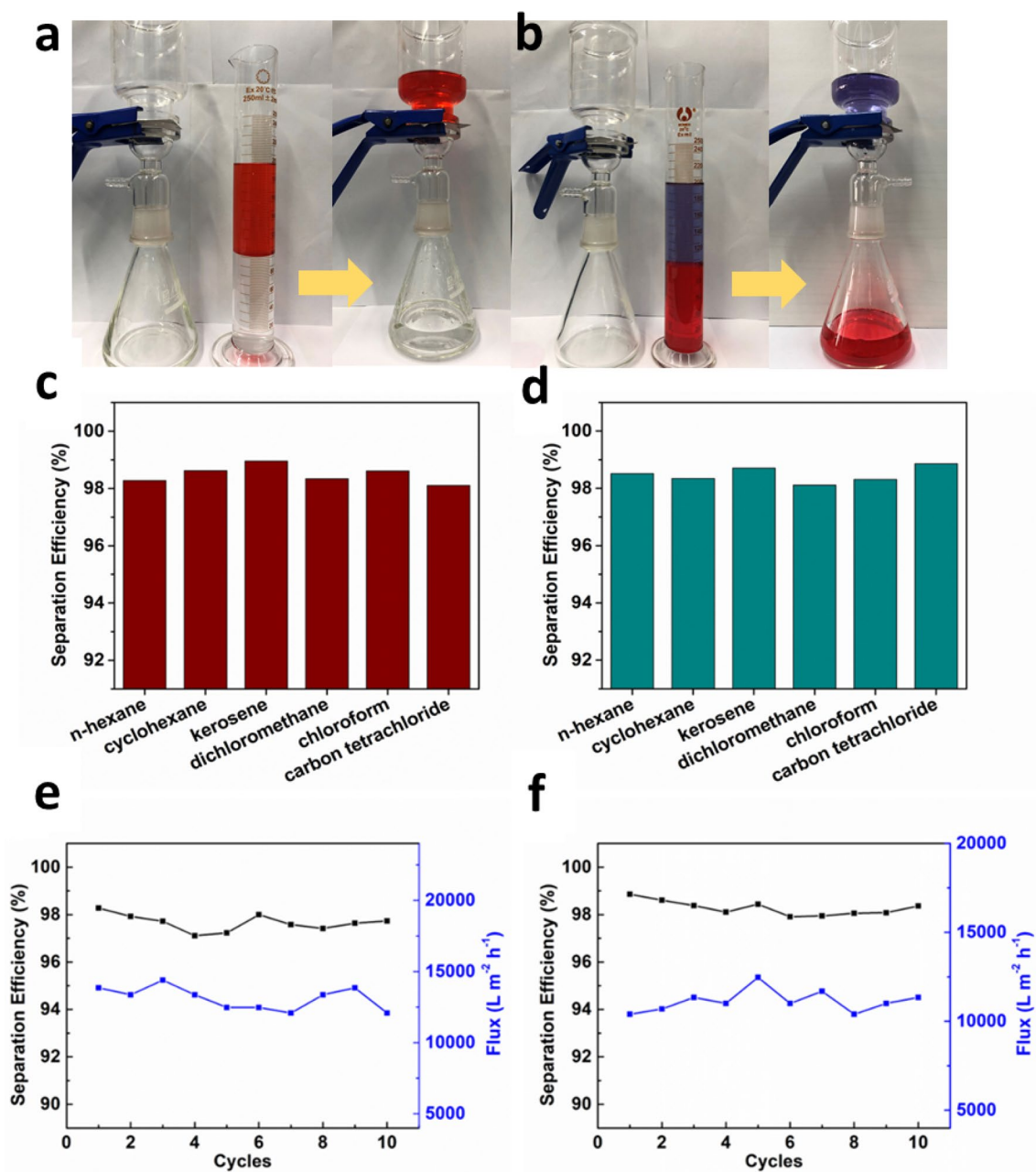
Fig. 5 Oil/water separation process of (**a**) *n*-hexane/acidic water mixture and (**b**) dichloromethane/alkaline water mixture. The oil used were dyed with Oil Red O. SE of different oil/solvents mixed with (**c**) acidic water or (**d**) alkaline water. SE of (**e**) *n*-hexane/acidic water mixture and (**f**) carbon tetrachloride/alkaline water mixture at different cycles

To verify the durability of DPS meshes towards acidic and alkaline environments, we soaked the meshes into five various solvents (1 M HCl solution, 1 M NaOH solution, 1 M NaCl solution, hot water, ice water) for 12 h. After immersion, the WCAs were about 150 ± 1° and the SE were about 97 ± 0.5% (Fig. 9). These results proved that the DPS mesh showed good stability in harsh environments, the copolymer and SiO₂ coating didn't peel off significantly due to the adhesion of the PDA.

Oil/water separating materials are inevitably exposed to sunlight in outdoor use. As a part of sunlight, ultraviolet (UV) light may cause decrease in super-wettability and further worsen the oil/water separation performance. Thus, WCAs and SE changes of DPS meshes were studied after treatment of UV irradiation for various time from 6 to 24 h. As shown in Fig. 10, only a slight decrease was observed in both WCA and SE after exposure to UV-irradiation. The WCAs were about 151 ± 1° and the SE were above 97%

Fig. 6 FESEM imagines of DPS mesh after separating *n*-hexane/acidic water mixture for ten cycles: (**a**) magnified 500 times, (**b**) magnified 5000 times. PS mesh after separating *n*-hexane/acidic water mixture for three cycles: (**c**) magnified 500 times, (**d**) magnified 5000 times
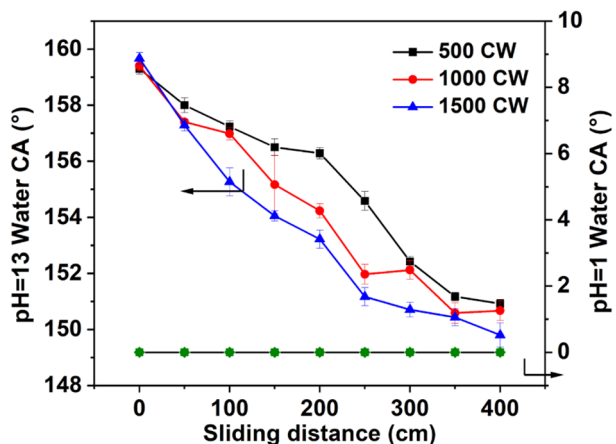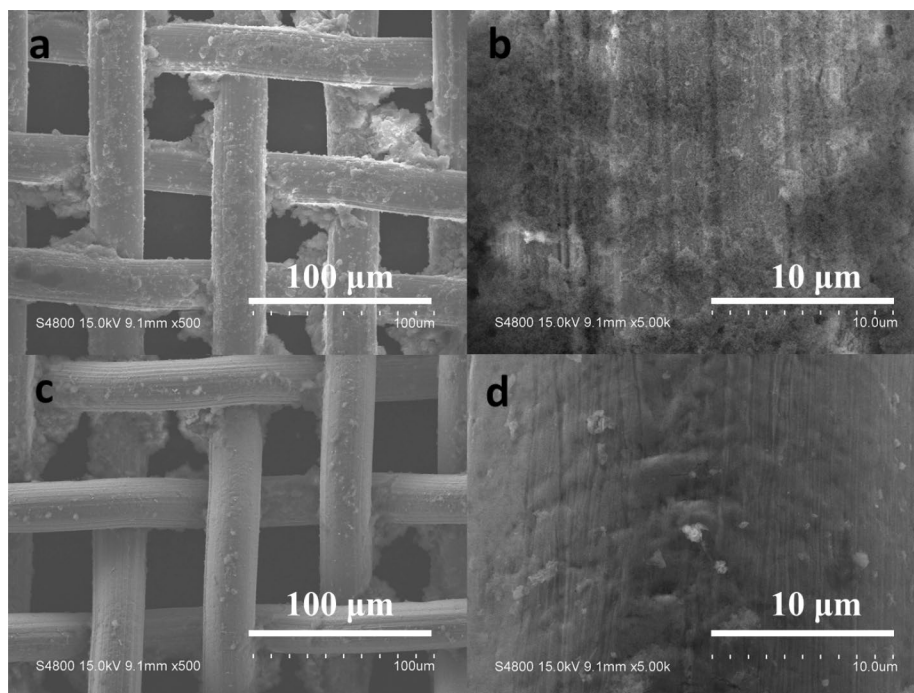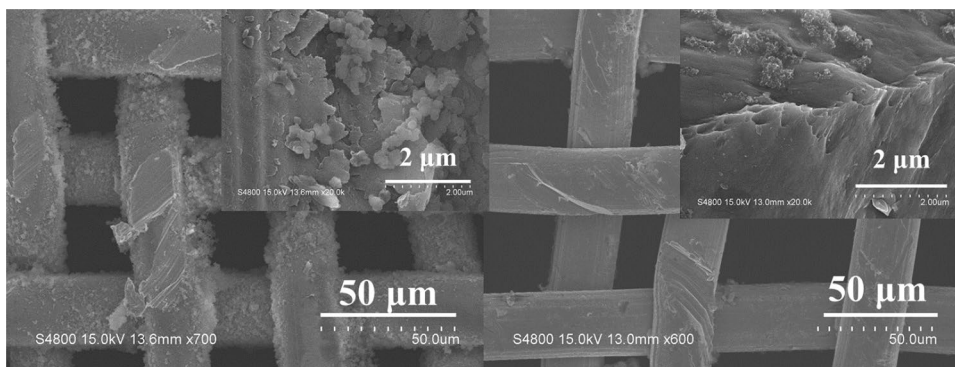

Fig. 7 WCA of DPS mesh after each 50 cm sliding distance on different sandpapers

Fig. 8 FESEM imagines of (**a**) DPS mesh and (**b**) PS mesh after 500 cm sliding distance on 500CW sandpaper

even after 24 h exposure. Hence, DPS mesh proved to be durable under UV irradiation, making it potentially conducive to long-term outdoor use.

Kapok fiber is a natural plant fiber with low density, good buoyancy, huge hollowness and good hydrophobicity. These characteristics endow kapok fiber higher oil sorption performance than common natural materials and commercial oil sorbent [53, 54]. Pristine kapok fiber assembly is difficult to retain oils effectively due to its smooth wax-covered surface and pectin coatings (Fig. S4). To remove the coatings, the kapok fiber was pretreated with NaClO$_2$ solution. In this work, we designed an oil collector with kapok fibers and DPS meshes. The as-prepared oil collector was placed on neutral water/Red O dyed *n*-hexane (Fig. 11a). *n*-Hexane passed through the mesh and was absorbed by the oil collector within a few seconds, leaving
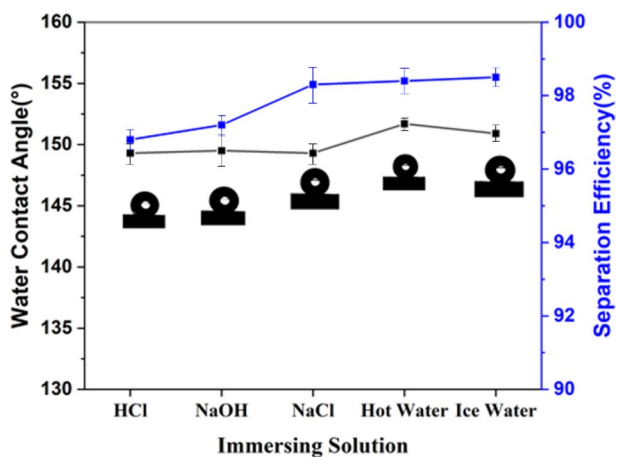
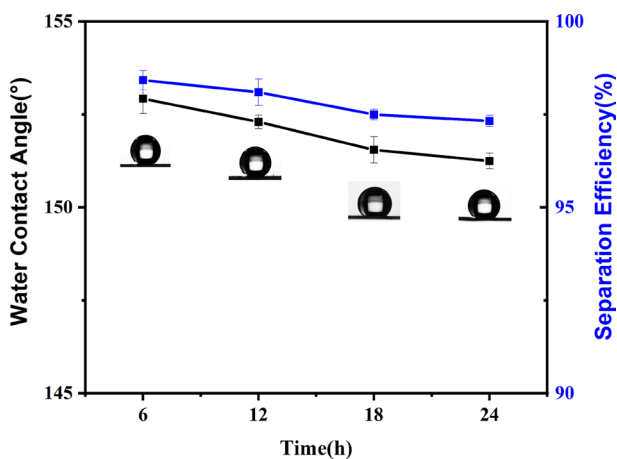**Fig. 9** The WCA and SE of DPS mesh after immersion into different solutions

Fig. 10 The WCA and SE of DPS mesh after treatment of UV irradiation for various time from 6 to 24 h
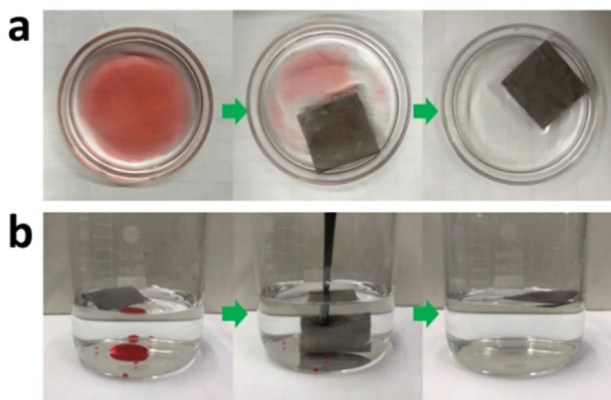

Fig. 11 Optical images of the process of DPS mesh selectively absorb (**a**) light oil (*n*-hexane) and (**b**) heavy oil (dichloromethane)
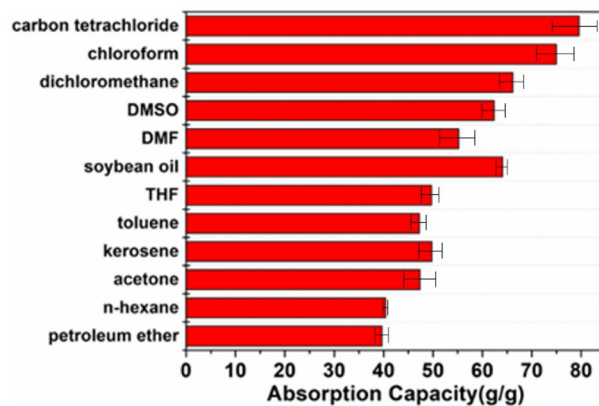
Fig. 12 Absorption capacity of oil collector to oil/solvent

the clear water phase without any visible oil droplets. The superhydrophobicity of the DPS mesh and the oleophilicity of kapok fibers in neutral environment played the vital role. Besides, the oil collector can also absorb heavy oil in water (Fig. 11b). At first, the oil collector floated on water in a hydrophobic situation. Once the oil collector was pressed into water and contacted the oil, the oil was quickly absorbed. The collector showed excellent selective absorption performance for the oil phase in water.

Moreover, the collector filled with 0.05 g of fiber assembly was used to evaluate the absorption capacities for twelve types of common oil pollutants in daily life and industry. As shown in Fig. 12, the absorption capacities of the oil collector for these oils were in the range of 39.67–79.56 g/g, much higher than some other oil-absorbing materials such as a biomimetic polypropylene foam (9.4 g/g) [55], electrospinning carbon nanofibrous membrane (44.9 g/g) [56] and [ADT-$(CF_3)_2$] modified polyurethane sponge (35.0–77.2 g/g) [57].

4 Conclusion

In summary, a durable DPS stainless steel mesh has been successfully fabricated by dip-coating of mesh into PDA solution and random copolymer suspension containing SiO_2 nanoparticles. The DPS mesh is pH-switchable wettability between superhydrophilicity-superoleophobicity and superhydrophobicity-superoleophilicity. The resulted mesh exhibited remarkable oil/water SE ≥ 98%) and desirable recyclability. The WCA of DPS mesh was about 150 ± 1° and the SE remained above 96% after abrasion test, acidic/alkali solution immersion and UV irradiation, exhibiting good durability in harsh environments compared with PS mesh due to the strong adhesion of PDA. Furthermore, an oil collector with excellent oil absorption capacity (39.67–79.56 g/g) was developed by as-prepared mesh

and kapok fiber. The facile fabrication, switchable wettability, together with excellent durable stability, made the DPS mesh promising in large-scale oil/water separation.

Compliance with ethical standards

Conflict of interest The authors declare that they have no conflict of interest.

References

1. Li JJ, Zhou YN, Luo ZH (2018) Polymeric materials with switchable superwettability for controllable oil/water separation: a comprehensive review. Prog Polym Sci 87:1–33
2. Yue XJ, Li ZD, Zhang T, Yang DY, Qiu FX (2019) Design and fabrication of superwetting fiber-based membranes for oil/water separation applications. Chem Eng J 364:292–309
3. Nanda D, Sahoo A, Kumar A, Bhushan B (2019) Facile approach to develop durable and reusable superhydrophobic/superoleophilic coatings for steel mesh surfaces. J Colloid Interf Sci 535:50–57
4. Panda A, Varshney P, Mohapatra SS, Kumar A (2018) Development of liquid repellent coating on cotton fabric by simple binary silanization with excellent self-cleaning and oil-water separation properties. Carbohyd Polym 181:1052–1060
5. Sun N, Zhu ZG, Zeng GF (2020) Bioinspired superwetting fibrous skin with hierarchical roughness for efficient oily water separation. Sci Total Environ 744:140822
6. Lei TP, Lu DH, Xu ZJ, Xu WK, Liu J, Deng XD, Huang JJ, Xu L, Cai XM, Lin LW (2020) 2D -> 3D conversion of superwetting mesh: a simple but powerful strategy for effective and efficient oil/water separation. Sep Purif Technol 242:116244
7. Wang RX, Zhao XT, Lan YY, Liu LF, Gao CJ (2020) In situ metal-polyphenol interfacial assembly tailored superwetting PES/SPES/MPN membranes for oil-in-water emulsion separation. J Membr Sci 615:118566
8. Dunderdale GJ, England MW, Sato T, Urata C, Hozumi A (2016) Programmable oil/water separation meshes: water or oil selectivity using contact angle hysteresis. Macromol Mater Eng 301(9):1032–1036
9. Tudu BK, Gupta V, Kumar A, Sinhamahapatra A (2020) Freshwater production via efficient oil-water separation and solar-assisted water evaporation using black titanium oxide nanoparticles. J Colloid Interf Sci 566:183–193
10. Bi YC, Wang ZY, Lu LL, Niu XM, Gu YB, Wang LN (2019) A facile route to engineer highly superhydrophobic antibacterial film through polymerizable emulsifier. Prog Org Coat 133:387–394
11. Yan T, Chen XQ, Zhang TH, Yu JG, Jiang XY, Hu WJH, Jiao FP (2018) A magnetic pH-induced textile fabric with switchable wettability for intelligent oil/water separation. Chem Eng J 347:52–63
12. Qu MN, Liu Q, He JM, Li JH, Liu LL, Yang C, Yang X, Peng L, Li KS (2020) A multifunctional superwettable material with excellent pH-responsive for controllable in situ separation multiphase oil/water mixture and efficient separation organics system. Appl Surf Sci 515:145991
13. Guo JH, Wang JK, Gao YH, Wang J, Chang WB, Liao SY, Qian ZM, Liu YX (2017) pH-responsive sponges fabricated by Ag–S ligands

14. possess smart double-transformed superhydrophilic-superhydrophobic-superhydrophilic wettability for oil-water separation. ACS Sustain Chem Eng 5(11):10772–10782
14. Ge MZ, Cao CY, Huang JY, Zhang XN, Tang YX, Zhou XR, Zhang KQ, Chen Z, Lai YK (2018) Rational design of materials interface at nanoscale towards intelligent oil-water separation. Nanoscale Horiz 3(3):235–260
15. Li JJ, Zhou YN, Luo ZH (2017) Mussel-inspired V-shaped copolymer coating for intelligent oil/water separation. Chem Eng J 322:693–701
16. Ge B, Yang XW, Li HY, Zhao LM, Ren GN, Miao X, Pu XP, Li WZ (2020) A durable superhydrophobic BiOBr/PFW cotton fabric for visible light response degradation and oil/water separation performance. Colloid Surf A 585:124027
17. Zhu HG, Yang S, Chen DY, Li NJ, Xu QF, Li H, He JH, Lu JM (2016) A robust absorbent material based on light-responsive superhydrophobic melamine sponge for oil recovery. Adv Mater Interfaces 3(5):1500683
18. Ge B, Ren GN, Yang H, Yang JJ, Pu XP, Li WZ, Jin CY, Zhang ZZ (2020) Fabrication of BiOBr-silicone aerogel photocatalyst in an aqueous system with degradation performance by sol-gel method. Sci China Technol Sci 63(5):859–865
19. Ngang HP, Ahmad AL, Low SC, Ooi BS (2017) Preparation of thermoresponsive PVDF/SiO2-PNIPAM mixed matrix membrane for saline oil emulsion separation and its cleaning efficiency. Desalination 408:1–12
20. Li D, Niu XQ, Yang SY, Chen YH, Ran F (2018) Thermo-responsive polysulfone membranes with good anti-fouling property modified by grafting random copolymers via surface-initiated eATRP. Sep Purif Technol 206:166–176
21. Zheng X, Guo ZY, Tian DL, Zhang XF, Jiang L (2016) Electric field induced switchable wettability to water on the polyaniline membrane and oil/water separation. Adv Mater Interfaces 3(18):1600461
22. Du L, Quan X, Fan XF, Chen S, Yu HT (2019) Electro-responsive carbon membranes with reversible superhydrophobicity/superhydrophilicity switch for efficient oil/water separation. Sep Purif Technol 210:891–899
23. Che HL, Huo M, Peng L, Fang T, Liu N, Feng L, Wei Y, Yuan JY (2015) CO2-responsive nanofibrous membranes with switchable oil/water wettability. Angew Chem Int Edit 54(31):8934–8938
24. Hu L, Gao SJ, Zhu YZ, Zhang F, Jiang L, Jin J (2015) An ultrathin bilayer membrane with asymmetric wettability for pressure responsive oil/water emulsion separation. J Mater Chem A 3(46):23477–23482
25. Kawamura T, Takeshita K (2020) Selective separation of Cd(II) and Am(III) by coating pH-responsive hydrophilic gel on silica particles. Sep Sci Technol. https://doi.org/10.1080/01496395.2020.1722168
26. Li Y, Zhu CH, Fan DD, Fu RZ, Ma P, Duan ZG, Li X, Lei H, Chi L (2020) Construction of porous sponge-like PVA-CMC-PEG hydrogels with pH-sensitivity via phase separation for wound dressing. Int J Polym Mater Polym Biomater 69(8):505–515
27. Shami Z, Gharloghi A, Amininasab SM (2019) Multifunctional pH-switched superwetting copolymer nanotextile: surface engineered toward on-demand light oil-water separation on superhydrophilic-underwater low-adhesive superoleophobic nonwoven mesh. ACS Sustain Chem Eng 7(9):8917–8930
28. Zhang ZB, Yu H, Guo JH, Bai ZW, Zhang SP, Zhang YJ, Wang JK (2019) pH-Responsive smart non-woven fabrics (NWFs) with double switchable wettability between superhydrophilicity-superhydrophobicity-superhydrophilicity to oil/water separation. New J Chem 43(17):6712–6720
29. Zhang LB, Wang P (2013) Nanotechnology based smart surfaces with switchable superoleophilicity and superoleophobicity in

aqueous media: toward controllable oil/water separation. Abstr Paper Am Chem Soc 245. https://doi.org/10.1038/am.2012.14

30. Zhang LB, Zhang ZH, Wang P (2012) Smart surfaces with switchable superoleophilicity and superoleophobicity in aqueous media: toward controllable oil/water separation. Npg Asia Mater 4:e8

31. Zhang QL, Xia F, Sun TL, Song WL, Zhao TY, Liu MC, Jiang L (2008) Wettability switching between high hydrophilicity at low pH and high hydrophobicity at high pH on surface based on pH-responsive polymer. Chem Commun (10):1199–1201

32. Dai GC, Zhang ZT, Du WN, Li ZJ, Gao WW, Li LX (2019) Conversion of skin collagen fibrous material waste to an oil sorbent with pH-responsive switchable wettability for high-efficiency separation of oil/water emulsions. J Clean Prod 226:18–27

33. Yi G, Fan XF, Quan X, Zhang HG, Chen S, Yu HT (2019) A pH-responsive PAA-grafted-CNT intercalated RGO membrane with steady separation efficiency for charged contaminants over a wide pH range. Sep Purif Technol 215:422–429

34. Li BC, Li LX, Wu L, Zhang JP, Wang AQ (2014) Durable superhydrophobic/superoleophilic polyurethane sponges inspired by Mussel and Lotus leaf for the selective removal of organic pollutants from water. Chempluschem 79(6):850–856

35. Lee H, Dellatore SM, Miller WM, Messersmith PB (2007) Mussel-inspired surface chemistry for multifunctional coatings. Science 318(5849):426–430

36. Chen K, Xu XQ, Guo JW, Zhang XL, Han SL, Wang RB, Li XH, Zhang JX (2015) Enhanced intracellular delivery and tissue retention of nanoparticles by mussel-inspired surface chemistry. Biomacromolecules 16(11):3574–3583

37. Heng CN, Liu MY, Wang K, Zheng XY, Huang HY, Deng FJ, Hui JF, Zhang XY, Wei Y (2015) Fabrication of silica nanoparticle based polymer nanocomposites via a combination of mussel inspired chemistry and SET-LRP. RSC Adv 5(111):91308–91314

38. Wan Q, Tian JW, Liu MY, Zeng GJ, Huang Q, Wang K, Zhang QS, Deng FJ, Zhang XY, Wei Y (2015) Surface modification of carbon nanotubes via combination of mussel inspired chemistry and chain transfer free radical polymerization. Appl Surf Sci 346:335–341

39. Zhang XY, Zeng GJ, Tian JW, Wan Q, Huang Q, Wang K, Zhang QS, Liu MY, Deng FJ, Wei Y (2015) PEGylation of carbon nanotubes via mussel inspired chemistry: preparation, characterization and biocompatibility evaluation. Appl Surf Sci 351:425–432

40. Miao L, Yang Y, Tu YY, Lin SD, Hu JW, Du Z, Zhang M, Li Y (2017) Chiral resolution by polysulfone-based membranes prepared via mussel-inspired chemistry. React Funct Polym 115:87–94

41. Xi ZY, Xu YY, Zhu LP, Wang Y, Zhu BK (2009) A facile method of surface modification for hydrophobic polymer membranes based on the adhesive behavior of poly(DOPA) and poly(dopamine). J Membr Sci 327(1–2):244–253

42. Zhao JJ, Su YL, He X, Zhao XT, Li YF, Zhang RN, Jiang ZY (2014) Dopamine composite nanofiltration membranes prepared by self-polymerization and interfacial polymerization. J Membr Sci 465:41–48

43. Zhan YQ, Wan XY, He SJ, Yang QB, He Y (2018) Design of durable and efficient poly(arylene ether nitrile)/bioinspired polydopamine coated graphene oxide nanofibrous composite membrane for anionic dyes separation. Chem Eng J 333:132–145

44. Feng XF, Yu ZX, Long RX, Sun YX, Wang M, Li XH, Zeng GY (2020) Polydopamine intimate contacted two-dimensional/

two-dimensional ultrathin nylon basement membrane supported RGO/PDA/MXene composite material for oil-water separation and dye removal. Sep Purif Technol 247:116945

45. Huang SY (2014) Mussel-inspired one-step copolymerization to engineer hierarchically structured surface with superhydrophobic properties for removing oil from water. ACS Appl Mater Inter 6(19):17144–17150

46. Kang HX, Zhao BW, Li LX, Zhang JP (2019) Durable superhydrophobic glass wool@polydopamine@PDMS for highly efficient oil/water separation. J Colloid Interf Sci 544:257–265

47. Jin L, Wang YJ, Xue T, Xie J, Xu YS, Yao Y, Li XX (2019) Smart amphiphilic random copolymer-coated sponge with pH-switchable wettability for on-demand oil/water separation. Langmuir 35(45):14473–14480

48. Song YP, Jin L, Guan XY, Wang CF, Lin XX (2020) Synthesis of pH-responsive polymer film and its application for oil/water separation. J East China Univ Sci Technol 46(01):33–40

49. Huang HW, Huang XF, Xie YH, Tian YQ, Jiang X, Zhang XY (2019) Fabrication of h-BN-rGO@PDA nanohybrids for composite coatings with enhanced anticorrosion performance. Prog Org Coat 130:124–131

50. Chen XL, Zhai YD, Han X, Liu HL, Hu Y (2019) Surface chemistry-dominated underwater superoleophobic mesh with mussel-inspired zwitterionic coatings for oil/water separation and self-cleaning. Appl Surf Sci 483:399–408

51. Jiang Y, Shi KX, Tang H, Wang YL (2019) Enhanced wettability and wear resistance on TiO2/PDA thin films prepared by sol-gel dip coating. Surf Coat Technol 375:334–340

52. Peng YX, Yu ZX, Li F, Chen Q, Yin D, Min X (2018) A novel reduced graphene oxide-based composite membrane prepared via a facile deposition method for multifunctional applications: oil/water separation and cationic dyes removal. Sep Purif Technol 200:130–140

53. Wang JT, Wang AQ, Wang WB (2017) Robustly superhydrophobic/superoleophilic kapok fiber with ZnO nanoneedles coating: highly efficient separation of oil layer in water and capture of oil droplets in oil-in-water emulsions. Ind Crop Prod 108:303–311

54. Wang JT, Geng GH, Liu X, Han FL, Xu JX (2016) Magnetically superhydrophobic kapok fiber for selective sorption and continuous separation of oil from water. Chem Eng Res Des 115:122–130

55. Huang PK, Wu F, Shen B, Ma XH, Zhao YQ, Wu MH, Wang J, Liu ZH, Luo HB, Zheng WG (2019) Bio-inspired lightweight polypropylene foams with tunable hierarchical tubular porous structure and its application for oil-water separation. Chem Eng J 370:1322–1330

56. Mantripragada S, Gbewonyo S, Deng DY, Zhang LF (2020) Oil absorption capability of electrospun carbon nanofibrous membranes having porous and hollow nanostructures. Mater Lett 262:127069

57. Guselnikova O, Barras A, Addad A, Sviridova E, Szunerits S, Postnikov P, Boukherroub R (2020) Magnetic polyurethane sponge for efficient oil adsorption and separation of oil from oil-in-water emulsions. Sep Purif Technol 240:116627